approach involves treadmill training with partial body weight support.[7] However, this approach requires considerable involvement of a physical therapist, and generally, 3 therapists are required to induce movement of the paretic leg during the swing phase and to shift the patient's weight onto the stance limb.

The potentially positive common benefits of robotic gait training are that it involves repeatedly undergoing sufficient and accurate training for a prolonged period. Lokomat is the first robotic-driven gait orthosis with electromechanical drives to assist the walking movements of gait-impaired patients on a treadmill by supporting the body weight.[8,9] Husemann et al[10] compared a Lokomat group that received 30 minutes of robotic training with a control group that received 30 minutes of conventional physiotherapy. After 4 weeks of therapy, although there was no significant difference in walking ability between the groups, the walking ability in both groups as expressed by functional ambulation classification was significantly improved. The researchers reported that the Lokomat group demonstrated an advantage for robotic training over conventional physiotherapy in the improvement of gait abnormality and body tissue composition.[10] However, in a recent randomized controlled study[11] that compared robot-assisted locomotor training with therapist-assisted locomotor training in chronic stroke patients, the results indicated that greater improvements in speed and single limb stance time on the impaired leg were observed in subjects who received therapist-assisted locomotor training. Thus, the usefulness of robot-assisted rehabilitation is controversial.

The robot suit hybrid assistive limb (HAL)[12-15,a] is a new wearable robot that has a hybrid control system composed of 2 subsystems: cybernic voluntary control (CVC) and cybernic autonomous control (CAC) (fig 1). The HAL suit has power units and force-pressure sensors in the shoes. The power units consist of angular sensors and actuators on bilateral hip and knee joints. Muscle action potentials are detected through the electrodes on the anterior and posterior surface of the wearer's thigh. These various biologic signals are processed by a computer. The HAL suit can support the wearer's motion by adjusting the level and timing of the assistive torque provided to each joint according to the surface muscle action potential as well as the pressure sensors. The HAL suit can enhance the wearer's motion through the wearer's muscle action potential; thus, the HAL suit can appear as an actual motion. Therefore, if the wearer's muscle action potential varies, the wearer's motion varies, too. The HAL training, using muscle activity, has the potential to intensify the feedback by inducing an appropriate motion more strongly than standard robot training. Thus, after HAL training, patients with limited mobility will improve their walking abilities (gait speed, number of steps, cadence, or ability to transfer).

Few studies have been conducted to clarify the feasibility of rehabilitation with HAL. Only 1 preliminary study[16] has reported on the short-term effects of HAL on the walking pattern of stroke patients. The purpose of the present study was to investigate the feasibility of 16-session (8-wk) HAL rehabilitation training for patients with limited mobility.

List of abbreviations:

BBS	Berg Balance Scale
CAC	cybernic autonomous control
CVC	cybernic voluntary control
HAL	hybrid assistive limb
MADS	musculoskeletal ambulation disability symptom complex
SCI	spinal cord injury
10MWT	10-m walk test
TUG	Timed Up & Go

Methods

Study design

A quasiexperimental study was used, with measurements before and after the clinical intervention. The target population included patients with limitations in their walking (no matter the diagnosis, the time since the diagnosis, and the patient's age at diagnosis). The protocol of this study was approved by the Institutional Review Board of the University of Tsukuba Hospital and was registered with the UMIN Clinical Trials Registry. The clinical intervention was conducted at the University of Tsukuba Hospital and Cyberdyne, Inc, in Japan between January 2010 and March 2012. The patients included in this study were volunteers recruited through local newspaper advertisements or outpatients at the University of Tsukuba Hospital. They were informed about the aim and design of this study, and they subsequently provided written, informed consent. Informed consent was also obtained from the patient's guardian if the patient was younger than 20 years.

The inclusion criteria were (1) musculoskeletal ambulation disability symptom complex (MADS) or the underlying disorders of MADS, which is a condition newly defined in 2006 by Japanese medical societies[17]; (2) requiring physical assistance or assistive devices in at least 1 of the following daily activities: standing up, sitting down, and walking; (3) ability to understand an explanation of the study and to express consent or refusal; (4) body size that can fit in the robotic suit HAL (height range, 145–180cm; maximal body weight, 80kg); and (5) ability to undergo usual physical and occupational therapies. The exclusion criteria were the following: (1) inadequately controlled cardiovascular disorders; (2) inadequately controlled respiratory disorders; (3) intellectual impairments that limit the ability to understand instructions; (4) moderate to severe articular disorders, including contracture in the lower extremities; (5) moderate to severe involuntary movements, ataxia, or impairments of postural reflex in the trunk or the lower extremities; and (6) severe spasticity in the lower extremities.

Participants

Thirty-eight patients (25 men, 13 women) were enrolled in this study (24 outpatients, 14 volunteers through advertisements). The mean age ± SD of the 38 patients was 53.2±17.8 years (range, 18–81y). Table 1 summarizes their clinical characteristics. Their underlying diseases were stroke (10 men, 2 women), SCI (6 men, 2 women), musculoskeletal diseases (2 men, 2 women), and other diseases (Parkinson's disease, gonadotropin-dependent myopathy, limb-girdle muscular dystrophy, inclusion body myositis, traumatic brain injury, disuse syndrome secondary to malignant lymphoma, cerebral palsy, sequelae of poliomyelitis, and hypoxic-ischemic encephalopathy; 7 men, 7 women). Twenty patients were able to ambulate independently without any help (n=9) or with several assistive devices (T-cane, bilateral crutches, or lateral crutch) (n=11). Eleven patients were able to ambulate with several assistive devices and under supervision. Three patients required human assistance to ambulate at least 10m (cases 33, 34, 38), and the remaining 4 patients were unable to ambulate even

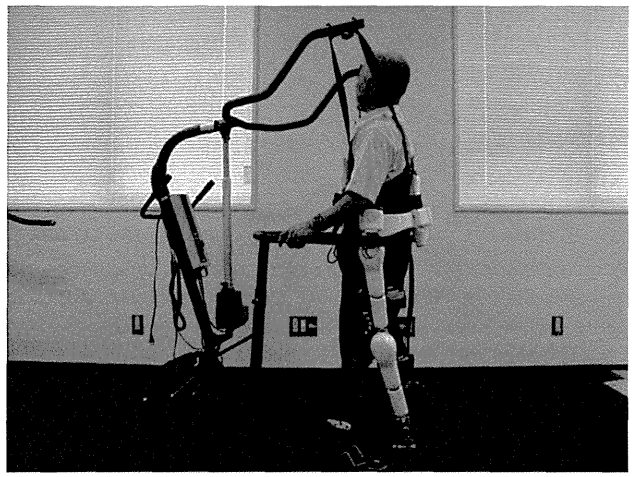

Fig 1 The robot suit HAL.

with assistive devices and human assistance (cases 8, 15, 17, 27). All the patients with stroke and SCI were in chronic stages.

Training program

HAL training was administered twice per week for 8 weeks (16 sessions). The 90-minute training sessions consisted of single-leg motion, a standing and sitting exercise, and walking on the ground with HAL. For safety reasons, a walking device (All-in-One Walking Trainer[b]) with a harness was used. Treadmill training with mild body-weight support (Unweighing System[c]) was also used for some patients. The HAL suit has a hybrid control system comprising the CVC and CAC. The CVC mode of the HAL suit can support the patient's voluntary motion according to the voluntary muscle activity and the assistive torque provided to each joint. The CAC mode provides physical support autonomously, based on output from force-pressure sensors in the shoes. This study mainly used the CVC mode, which allows the operator to adjust the degree of physical support to the patient's comfort and gradually reduce support as training progresses.

Outcome measures

The feasibility of rehabilitation with HAL was assessed by the number of completers and the amount of time or the number of therapists needed to implement training. Patients were asked to report adverse events during the training period.

The primary outcomes were functional ambulation and balance ability. Functional ambulation was assessed with a 10-m walk test (10MWT) and a Timed Up & Go (TUG) test. In the 10MWT, patients were instructed to walk without wearing HAL on a flat surface at their self-selected, comfortable pace. Patients began to walk before they reached the starting line of the 10-m distance so that they could accelerate and attain a stable speed before the test. To calculate gait speed (m/s) as a primary outcome, the 10-m walking time was measured using a handheld stopwatch. In addition, the number of steps between the start and finish line was counted, and patient cadence was calculated from the walking time and number of steps. Patients were allowed to use their assistive device or lower limb orthosis, or both, as necessary. Each patient used the same assistive device or orthosis, or both, during the pre- and postintervention measurements. Therapists closely attended the patients during the 10MWT but did not provide physical assistance. For each measurement, the 10MWT was performed twice. The faster time of 2 trials was selected for analysis. In the TUG test, the following actions were timed: standing up from a standard-height chair, walking 3m, returning to the chair, and sitting down without HAL. Two trials (each turning clockwise and counterclockwise) were carried out for each measurement. Balance ability was assessed with the Berg Balance Scale (BBS), consisting of 14 tasks, as detailed by Berg et al.[18] Each task was scored on a scale ranging from 0 to 4 points (0 indicates inability to complete), and the total score was used as the index of balance ability. All primary outcomes were assessed at baseline and after completion of the 16 training sessions.

Statistical analysis

All parametric data are expressed as means with SDs. Paired *t* tests were used to evaluate differences between the baseline measurements and outcomes after the 16 sessions. Unpaired *t* tests were used to evaluate the differences in characteristics of those who completed 16 sessions and those who did not. An effect-size calculation (Cohen *d*) was used to assess the effect of the training. Pearson correlation coefficients were used to assess the relationship among outcome measures. Data were analyzed using IBM SPSS Statistics 18 software,[d] with the alphas level set at 5%.

Results

A typical 90-minute HAL training session proceeded as follows: assessment of blood pressure, resting heart rate, and walking pattern (10min); preparation of electrodes and putting on the HAL suit (5min); computer setup (5min); HAL training (60min, including resting time during computer operation); taking off the HAL suit and the electrodes (5min); and reassessment of walking pattern (5min). The net walking time was approximately 20 minutes. Typically, 2 therapists implemented the training: one supported the patient and the other operated the computer. All therapists and related staff had participated in a 3-hour training workshop conducted by the manufacturer to learn how to operate the HAL system.

Of the 38 patients (25 men, 13 women), 32 (21 men, 11 women) completed all 16 training sessions. The mean age ± SD of the 32 patients was 53.2±17.3 years (range, 18–81y). There was no statistically significant difference in age between those who completed training and those who did not (54.0±19.8y). It took 10.0±3.1 weeks (range, 8–21wk) to complete 16 sessions. Of the 6 patients who did not complete the 16 sessions, 2 (cases 15, 21) dropped out for medical reasons, and 4 (cases 1, 2, 29, 35) dropped out for personal reasons (difficulty visiting the hospital). One medical reason for dropout was low back pain that developed during the first training session (case 21); the patient withdrew consent at the third session. The other medical reason for dropout was a relapse (after the second session) of neuropathic pain caused by SCI (case 15); the patient withdrew consent at the fifth session. There were no serious training-related adverse events. One stroke patient (case 7) had knee pain (patellar tendinitis) at home after the 15th session but was able to complete the 16th session after 1 month of rest. Another patient with inclusion body myositis (case 31) developed knee

Table 1 Clinical characteristics of patients

Case No.	Age (y)	Sex	Diagnosis	Paralysis Type	Duration Since Disease	Ambulation	Assistive Device	Orthosis	Training	Duration of Training (wk)	Adverse Events
1	69	M	Stroke (cerebral infarcts)	Paraplegia	15y	Independently	T-cane	AFO	Dropout (personal reason)	ND	Nothing
2	61	M	Stroke (cerebral hemorrhage)	Paraplegia	14y8mo	Independently	T-cane	AFO	Dropout (personal reason)	ND	Nothing
3	65	M	Stroke (cerebral hemorrhage)	Hemiplegia	2y2mo	Supervision	Quad-cane	AFO	Complete	8	Nothing
4	37	F	Stroke (cerebral hemorrhage)	Quadriplegia	16y	Independently	NA	AFO	Complete	8	Nothing
5	72	M	Stroke (cerebral infarcts)	Hemiplegia	2y9mo	Supervision	T-cane	AFO	Complete	8	Nothing
6	54	M	Stroke (cerebral hemorrhage)	Hemiplegia	1y1mo	Supervision	T-cane	NA	Complete	8	Nothing
7	63	F	Stroke (cerebral hemorrhage)	Hemiplegia	1y6mo	Independently	T-cane	AFO	Complete	15	Knee pain (patellar tendinitis)
8	52	M	Stroke (cerebral hemorrhage)	Ataxia	2y2mo	NA	NA	NA	Complete	12	Nothing
9	74	M	Stroke (cerebral infarcts)	Hemiplegia	3y4mo	Independently	T-cane	AFO	Complete	9	Nothing
10	53	M	Stroke (subarachnoid hemorrhage, cerebral infarcts)	Hemiplegia	ND	Supervision	Pick-up walker	KAFO	Complete	9	Nothing
11	18	M	Stroke (moyamoya disease)	Hemiplegia	11y	Independently	NA	AFO	Complete	21	Nothing
12	64	M	Stroke (cerebral hemorrhage)	Hemiplegia	1y	Supervision	T-cane	AFO	Complete	8	Nothing
13	58	F	SCI (incomplete)	Quadriplegia	3y3mo	Supervision	Lateral crutch	KAFO	Complete	8	Nothing
14	69	M	SCI (incomplete)	Quadriplegia	1y3mo	Supervision	Pick-up walker	AFO	Complete	8	Nothing
15	43	M	SCI (incomplete)	Paraplegia	3y3mo	NA	NA	KAFO	Dropout (medical reason)	ND	Neuropathic pain after SCI
16	59	M	SCI (spina bifida)	Paraplegia	6y4mo	Supervision	T-cane	NA	Complete	8	Nothing
17	31	M	SCI (complete)	Paraplegia	3y	NA	NA	NA	Complete	10	Nothing
18	64	F	SCI (incomplete)	Quadriplegia	2y	Independently	T-cane	AFO	Complete	9	Nothing
19	54	M	SCI (central cervical cord injury)	Quadriplegia	5y	Supervision	T-cane	NA	Complete	12	Nothing
20	47	M	SCI (spinal dural arteriovenous fistula)	Paraplegia	1y1mo	Independently	Bilateral crutch	AFO	Complete	8	Nothing
21	74	F	Musculoskeletal disease (cervical spondylotic myelopathy)	Quadriplegia	ND	Independently	Bilateral crutch	NA	Dropout (medical reason)	ND	Low back pain
22	81	F	Musculoskeletal disease (OA knee)	NA	ND	Independently	NA	NA	Complete	10	Nothing
23	44	M	Musculoskeletal disease (OA knee)	NA	ND	Independently	NA	NA	Complete	11	Nothing
24	74	M	Musculoskeletal disease (OA knee)	NA	ND	Independently	NA	NA	Complete	10	Nothing
25	62	M	Parkinson's disease	NA	8y	Independently	NA	NA	Complete	11	Nothing

(*continued on next page*)

Table 1 (*continued*)

Case No.	Age (y)	Sex	Diagnosis	Paralysis Type	Duration Since Disease	Ambulation	Assistive Device	Orthosis	Training	Duration of Training (wk)	Adverse Events
26	72	F	Parkinson's disease	NA	7y8mo	Independently	Nothing	NA	Complete	9	Nothing
27	36	M	Gonadotropin-dependent myopathy	Paraplegia	19y	NA	NA	NA	Complete	8	Nothing
28	52	F	Limb-girdle muscular dystrophy	Quadriplegia	24y	Supervision	T-cane	NA	Complete	9	Nothing
29	57	F	Muscular dystrophy	NA	44y	Independently	NA	NA	Dropout (personal reason)	ND	Nothing
30	67	M	Limb-girdle muscular dystrophy	NA	28y	Independently	T-cane	NA	Complete	8	Nothing
31	73	M	Inclusion body myositis	NA	10y	Independently	T-cane	NA	Complete	10	Knee pain
32	24	M	Traumatic brain injury	Quadriplegia	17y1mo	Supervision	Walker	NA	Complete	8	Nothing
33	19	F	Traumatic brain injury	Quadriplegia	6y2mo	Assistance	Pick-up walker	KAFO	Complete	8	Nothing
34	29	F	Traumatic brain injury	Quadriplegia	10y7mo	Assistance	Pick-up walker	KAFO	Complete	9	Nothing
35	20	M	Disuse syndrome, secondary to malignant lymphoma	NA	3y9mo	Independently	T-cane	NA	Dropout (personal reason)	ND	Nothing
36	31	F	Cerebral palsy	Quadriplegia	30y10mo	Independently	Lateral crutch	NA	Complete	10	Nothing
37	55	M	Sequelae of poliomyelitis	Paraplegia	54y	Independently	Lateral crutch	NA	Complete	19	Nothing
38	48	F	Hypoxic-ischemic encephalopathy	Quadriplegia	2y	Assistance	NA	NA	Complete	12	Nothing

Abbreviations: AFO, ankle-foot orthosis; F, female; KAFO, knee-ankle-foot orthosis; M, male; NA, not applicable; ND, no data; OA, osteoarthritis.

Table 2 Functional ambulation and balance ability at baseline and after 16-session HAL training

Outcome Measurements	Baseline	After Training	Difference	*P*	n
10MWT					
Speed (m/s)	0.52±0.40	0.61±0.43	0.09 (0.05 to 0.14)	<.001	27
No. of steps	34.0±20.4	31.0±18.8	−3.0 (−4.9 to −1.0)	<.001	27
Cadence (steps/min)	74.3±34.1	81.1±32.9	6.8 (4.0 to 9.6)	<.001	27
TUG (s)	43.7±45.0	37.3±34.1	−6.4 (−13.0 to 0.2)	.057	26
BBS	33.6±16.9	35.5±16.3	1.9 (−0.1 to 3.9)	.059	32

NOTE. Values are mean ± SD, mean (95% confidence interval), or as otherwise indicated.

pain at home after an early session but was able to complete 16 sessions.

Outcome measures

Functional ambulation was not assessed for 5 patients at baseline because 3 were unable to ambulate with any assistance (cases 8, 17, 27), and the other 2 patients needed considerable human assistance to ambulate (cases 34, 38). The other 27 patients had significant improvements ($P<.05$) in gait speed, number of steps, and cadence after the 16-session HAL training (10MWT, table 2). Improvements in gait speed, number of steps, and cadence are defined as an increase, a decrease, and an increase in the respective parameters. The mean ± SD improvements and effect sizes (Cohen *d*) in gait speed, number of steps, and cadence were .09±.11m/s ($d=.82$), 3.0±4.9 steps ($d=.61$), and 6.8±7.1 steps/min ($d=.96$), respectively. Improvements in gait speed, steps, and cadence were observed in 25, 18, and 25 patients, respectively (figs 2–4). Worsened gait speed and cadence were observed in 2 patients (cases 28, 30). In regards to the number of steps, we observed no change in 8 patients (cases 3, 5, 16, 25, 28, 30, 33, 37) and increased steps in 1 (case 20). Correlation coefficients for gait speed with number of steps and with cadence were $r=.30$ (not significant) and $r=.73$ ($P<.01$), respectively. The effect sizes for gait speed in patients with stroke (n=9), SCI (n=6), musculoskeletal disease (n=3), and patients with other diseases (n=9) were 1.41, .78, 2.43, and .63, respectively. The results of the TUG test (n=26; case 10 was unable to perform the test) and the BBS (n=32) indicated improvement after the 16 training sessions, but these improvements were not statistically significant. The mean ± SD decrease (Cohen *d*) in the TUG test was 6.4±16.4 seconds ($d=.39$). Twenty-one of 26 patients were faster after training, and 5 patients were slower (cases 5, 13, 30, 31, 36) (fig 5). The mean ± SD increase (Cohen *d*) in BBS was 1.9±5.5 ($d=.35$). Nineteen of 32 patients had higher scores compared with baseline; no change was observed in 6 (cases 12, 17, 23, 27, 36, 37), and 7 had lower scores (cases 11, 16, 26, 30, 31, 32, 34) (fig 6).

Discussion

We investigated the feasibility of rehabilitation using a robot suit HAL. We demonstrated that HAL rehabilitation could be implemented safely and effectively. Although a few patients developed lumbar or knee pain during the training, no serious training-related adverse events occurred. Significant improvements in gait speed, number of steps, and cadence were observed, as assessed by the 10MWT. Improved TUG test and BBS results were also observed, but because of the small sample size of this pilot study, these improvements were not statistically significant. Overall, our results suggest that HAL rehabilitation has the potential to improve ambulation in patients with limited mobility.

Two patients (cases 15, 21) dropped out for medical reasons. One developed lumbar pain (case 21), and 1 had a relapse of neuropathic pain caused by SCI (case 15). Although it is unclear

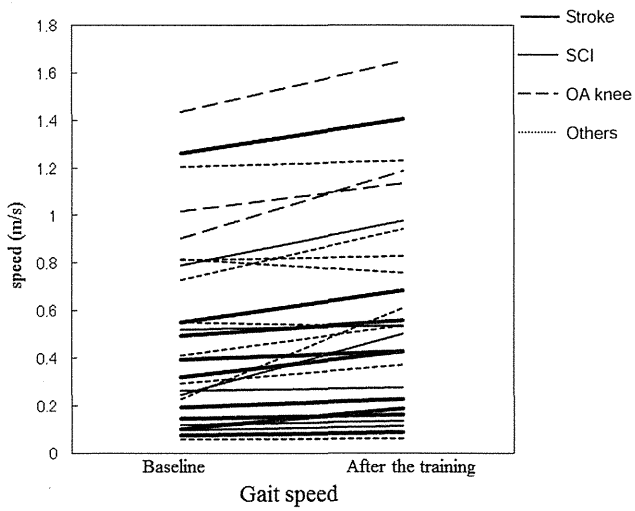

Fig 2 Change in 10MWT gait speed for 27 patients after HAL training. Abbreviation: OA, osteoarthritis.

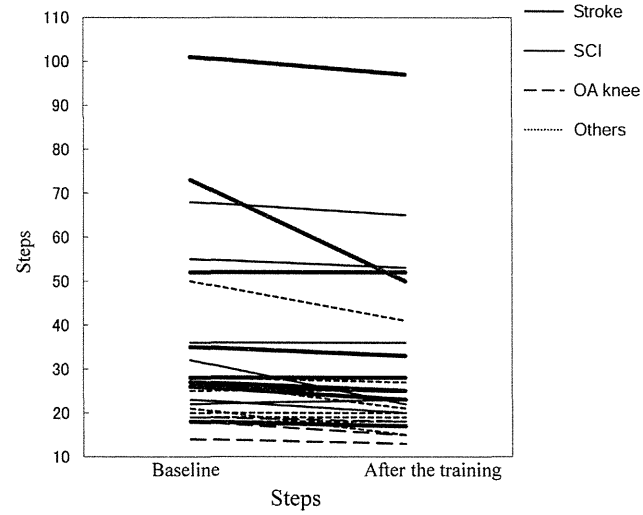

Fig 3 Change in number of steps during 10MWT for 27 patients after HAL training. Abbreviation: OA, osteoarthritis.

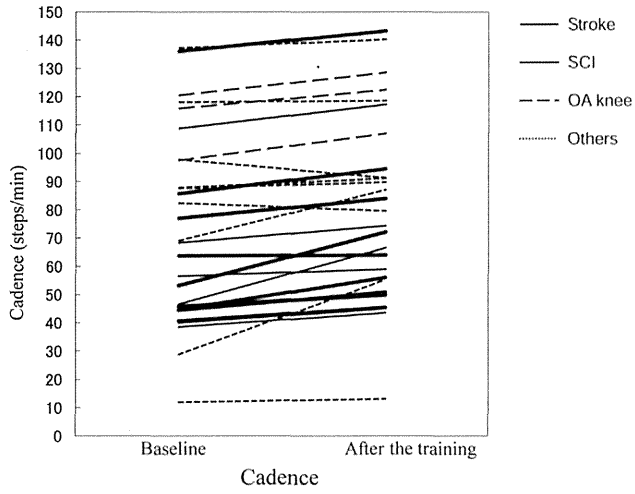

Fig 4 Change in 10MWT cadence for 27 patients after HAL training. Abbreviation: OA, osteoarthritis.

whether there was a causal relationship between HAL training and the pain that developed, the lumbar pain in case 21 had been persistent before the HAL training and even after the training ended, and the neuropathic pain in case 15 followed a previous pattern of symptom flares associated with seasonal change. Therefore, it is likely that HAL training did not directly cause the pain that developed in these 2 cases. Two other patients complained of knee pain during the training period, but this pain was not severe, and the patients were able to complete the training. Although, once again, direct causality is unclear, safe implementation of HAL rehabilitation requires adequate caution on the part of therapists and self-awareness on the part of patients who have lumbar and knee pain. Regarding feasibility, approximately 10 minutes was required for 2 to 3 therapists to put electrodes and the HAL suit on or take them off the patient. This procedure is a slight inconvenience to address but not a major obstacle to HAL rehabilitation.

Significant improvements in functional ambulation were observed, and the effect sizes (Cohen d) for gait speed, number of steps, and cadence were .82, .61, and .96, respectively. The correlation coefficient for gait speed with cadence was higher than

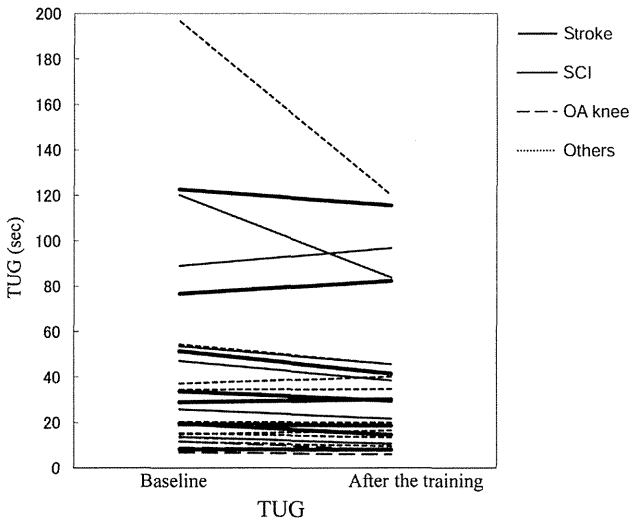

Fig 5 Change in TUG test results for 26 patients after HAL training. Abbreviation: OA, osteoarthritis.

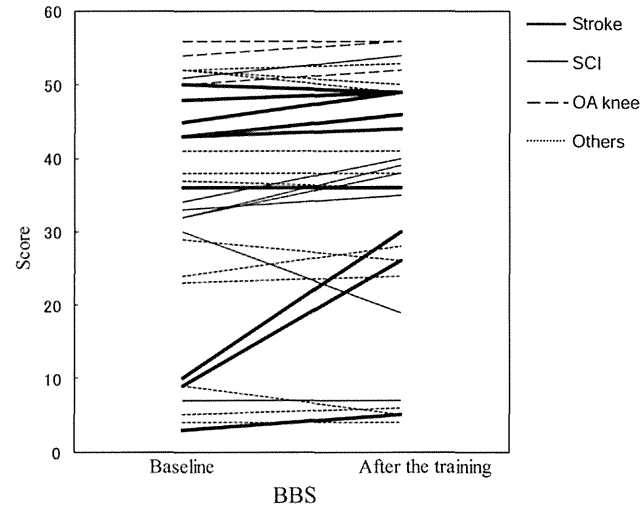

Fig 6 Change in BBS score for 32 patients after HAL training. Abbreviation: OA, osteoarthritis.

that of gait speed with steps (r=.73 vs r=.30). Therefore, the improvement in gait speed with HAL training was mainly brought about by improvement in cadence. That is, HAL training improved stride frequency more than stride length. This finding is in agreement with that of a previous robotic training study.[19] The effect sizes for the TUG test and BBS were smaller than the effect sizes for the 10MWT. This result seems to occur because the TUG test and BBS involve complicated motions such as moving from sitting to standing, walking and returning, reaching forward, and alternating feet on each step. The effect sizes for gait speed in 9 patients with stroke and in 6 patients with SCI were large (1.41 and .78, respectively). Therefore, training effectiveness in patients with stroke and those with SCI can be expected. The effect size in 3 patients with musculoskeletal diseases was also large (2.43), but the number of patients was small. Therefore, further studies are needed. In this study, we recruited patients with a wide range of stroke and SCI severities. Future studies should examine the influence of the severity of stroke and SCI on the effectiveness of HAL rehabilitation.

Many recent studies have reported the efficacy of robot-assisted rehabilitation. It is very difficult to directly compare these studies and our study, because of differences in diseases, severity and duration of the disorder, robotic features, methods of intervention, and outcome measures.[20] Wirz et al[21] reported that after locomotor training with Lokomat, the 10MWT gait speed of 20 patients with chronic incomplete SCI increased by .11±.10m/s (d=1.10). The number of patients with SCI in our study was limited to 6, but our results also indicate the efficacy of HAL rehabilitation for these patients (d=.78). Hornby et al[11] reported that after robotic-assisted locomotor training, the gait speed in chronic stroke patients increased by .07±.07m/s (d=1.0). Our results also indicate the efficacy of HAL rehabilitation for 9 patients with chronic stroke (d=1.41). We conjectured that the mechanism of this recovery of functional ambulation was due to changes in plasticity in the spinal cord and supraspinal centers. Appropriate sensory inputs, such as maximum weight loading, facilitating proper trunk posture, and hip extension, are essential for maximizing functional recovery.[22] Our experience with HAL indicates that the HAL-induced motion might evoke the sensory input, which has a favorable feedback effect on the central nervous system for a recovery of locomotor function. In addition, even if a patient's condition were too severe for medical therapists to

provide adequate rehabilitation training, HAL might still make adequate training possible. HAL is a robotic device with potential rehabilitation applications that are dependent on the physical support it can provide.

Study limitations

This study was not a randomized controlled trial and could not compare the efficacy of HAL training with conventional rehabilitation. Second, long-term efficacy was not assessed after HAL training. Third, this study could not exclude observer bias and subject bias because the same staff implemented assessment and training, and approximately half of the patients were recruited through local newspaper advertisements. Finally, the statistical power was low because of the small number of patients with each disease.

Conclusions

This quasiexperimental study revealed the feasibility of HAL training for rehabilitating patients with limited mobility. This study has shown that it is possible to manage 8 weeks of rehabilitation with HAL training (16 sessions of 90min) safely and effectively, even with persons who received their diagnosis many years ago. After HAL training, significant improvements in gait speed, number of steps, and cadence were observed. Although improvements were observed in the TUG test and BBS, they were not statistically significant. There were no serious adverse events. Further studies are needed to compare the effectiveness of HAL training and conventional rehabilitation.

Suppliers

a. Cyberdyne Inc, D25-1, Gakuen Minami, Tsukuba, Ibaraki, Japan 305-0818.
b. ROPOX A/S, 221 Ringstedgade, Naestved, Denmark 4700.
c. Biodex Medical Systems Inc, 20 Ramsay Rd, Shirley, NY 11967.
d. SPSS, Inc, 233 S Wacker Dr, 11th Fl, Chicago, IL 60606.

Keywords

Feasibility studies; Mobility limitation; Orthopedic equipment; Rehabilitation; Robotics

Corresponding author

Kiyoshi Eguchi, MD, PhD, Associate Professor, Dept of Rehabilitation Medicine, Faculty of Medicine, University of Tsukuba, 1-1-1 Tennodai, Tsukuba, Ibaraki 305-8575, Japan. *E-mail address:* kyeguchi@md.tsukuba.ac.jp.

Acknowledgments

We thank Kanako Yamawaki, Ryohei Ariyasu, and Aki Ichikawa, Center for Cybernics Research, University of Tsukuba, for their excellent technical assistance.

References

1. van Vliet P, Wing AM. A new challenge: robotics in the rehabilitation of the neurologically motor impaired. Phys Ther 1991;71:39-47.
2. Tefertiller C, Pharo B, Evans N, Winchester P. Efficacy of rehabilitation robotics for walking training in neurological disorders: a review. J Rehabil Res Dev 2011;48:387-416.
3. Colombo G, Joerg M, Schreier R, Dietz V. Treadmill training of paraplegic patients using a robotic orthosis. J Rehabil Res Dev 2000; 37:693-700.
4. Veneman JF, Kruidhof R, Hekman EE, Ekkelenkamp R, Van Asseldonk EH, van der Kooij H. Design and evaluation of the LOPES exoskeleton robot for interactive gait rehabilitation. IEEE Trans Neural Syst Rehabil Eng 2007;15:379-86.
5. Hesse S, Uhlenbrock D, Werner C, Bardeleben A. A mechanized gait trainer for restoring gait in nonambulatory subjects. Arch Phys Med Rehabil 2000;81:1158-61.
6. Schmidt H, Werner C, Bernhardt R, Hesse S, Kruger J. Gait rehabilitation machines based on programmable footplates. J Neuroeng Rehabil 2007;4:2.
7. Visintin M, Barbeau H, Korner-Bitensky N, Mayo NE. A new approach to retrain gait in stroke patients through body weight support and treadmill stimulation. Stroke 1998;29:1122-8.
8. Lünenburger L, Colombo G, Riener R, Dietz V. Biofeedback in gait training with the robotic orthosis Lokomat. Conf Proc IEEE Eng Med Biol Soc 2004;7:4888-91.
9. Neckel N, Wisman W, Hidler J. Limb alignment and kinematics inside a Lokomat robotic orthosis. Conf Proc IEEE Eng Med Biol Soc 2006; 1:2698-701.
10. Husemann B, Müller F, Krewer C, Heller S, Koenig E. Effects of locomotion training with assistance of a robot-driven gait orthosis in hemiparetic patients after stroke: a randomized controlled pilot study. Stroke 2007;38:349-54.
11. Hornby TG, Campbell DD, Kahn JH, Demott T, Moore JL, Roth HR. Enhanced gait-related improvements after therapist- versus robotic-assisted locomotor training in subjects with chronic stroke: a randomized controlled study. Stroke 2008;39:1786-92.
12. Kawamoto H, Sankai Y. Power assist method based on phase sequence and muscle force condition for HAL. Adv Robot 2005;19:717-34.
13. Lee S, Sankai Y. Virtual impedance adjustment in unconstrained motion for an exoskeletal robot assisting the lower limb. Abv Robot 2005;19:773-95.
14. Suzuki K, Gouji M, Kawamoto H, Hasegawa Y, Sankai Y. Intention-based walking support for paraplegia patients with robot suit HAL. Adv Robot 2007;21:1441-69.
15. Tsukahara A, Kawanishi R, Hasegawa Y, Sankai Y. Sit-to-stand and stand-to-sit transfer support for complete paraplegic patients with robot suit HAL. Adv Robot 2010;24:1615-38.
16. Maeshima S, Osawa A, Nishio D, et al. Efficacy of a hybrid assistive limb in post-stroke hemiplegic patients: a preliminary report. BMC Neurol 2011;11:116.
17. Michikawa T, Nishiwaki Y, Takebayashi T, Toyama Y. One-leg standing test for elderly populations. J Orthop Sci 2009;14(5):675-85.
18. Berg K, Wood-Dauphinee S, Williams JI. The balance scale: reliability assessment with elderly residents and patients with an acute stroke. Scand J Rehabil Med 1995;27:27-36.
19. Nooijen CF, Ter Hoeve N, Field-Fote EC. Gait quality is improved by locomotor training in individuals with SCI regardless of training approach. J Neuroeng Rehabil 2009;6:36.
20. Hachisuka K. [Robot-aided training rehabilitation] [Japanese]. Brain Nerve 2010;62(2):133-40.
21. Wirz M, Zemon DH, Rupp R, et al. Effectiveness of automated locomotor training in patients with chronic incomplete spinal cord injury: a multicenter trial. Arch Phys Med Rehabil 2005;86: 672-80.
22. Barbeau H. Locomotor training in neurorehabilitation: emerging rehabilitation concepts. Neurorehabil Neural Repair 2003;17:3-11.

Saito et al. Retrovirology 2013, 10:51
http://www.retrovirology.com/content/10/1/51

RETROVIROLOGY

RESEARCH Open Access

Increased expression of OX40 is associated with progressive disease in patients with HTLV-1-associated myelopathy/tropical spastic paraparesis

Mineki Saito[1,6*], Reiko Tanaka[1], Shiho Arishima[2], Toshio Matsuzaki[3], Satoshi Ishihara[4], Takashi Tokashiki[4], Yusuke Ohya[4], Hiroshi Takashima[3], Fujio Umehara[5], Shuji Izumo[2] and Yuetsu Tanaka[1]

Abstract

Background: OX40 is a member of the tumor necrosis factor receptor family that is expressed primarily on activated $CD4^+$ T cells and promotes the development of effector and memory T cells. Although OX40 has been reported to be a target gene of human T-cell leukemia virus type-1 (HTLV-1) viral transactivator Tax and is overexpressed *in vivo* in adult T-cell leukemia (ATL) cells, an association between OX40 and HTLV-1-associated inflammatory disorders, such as HTLV-1-associated myelopathy/tropical spastic paraparesis (HAM/TSP), has not yet been established. Moreover, because abrogation of OX40 signals ameliorates chronic inflammation in animal models of autoimmune disease, novel monoclonal antibodies against OX40 may offer a potential treatment for HTLV-1-associated diseases such as ATL and HAM/TSP.

Results: In this study, we showed that OX40 was specifically expressed in $CD4^+$ T cells naturally infected with HTLV-1 that have the potential to produce pro-inflammatory cytokines along with Tax expression. We also showed that OX40 was overexpressed in spinal cord infiltrating mononuclear cells in a clinically progressive HAM/TSP patient with a short duration of illness. The levels of the soluble form of OX40 (sOX40) in the cerebrospinal fluid (CSF) from chronic progressive HAM/TSP patients or from patients with other inflammatory neurological diseases (OINDs) were not different. In contrast, sOX40 levels in the CSF of rapidly progressing HAM/TSP patients were higher than those in the CSF from patients with OINDs, and these patients showed higher sOX40 levels in the CSF than in the plasma. When our newly produced monoclonal antibody against OX40 was added to peripheral blood mononuclear cells in culture, HTLV-1-infected T cells were specifically removed by a mechanism that depends on antibody-dependent cellular cytotoxicity.

Conclusions: Our study identified OX40 as a key molecule and biomarker for rapid progression of HAM/TSP. Furthermore, blocking OX40 may have potential in therapeutic intervention for HAM/TSP.

Keywords: HTLV-1, OX40, HAM/TSP, ADCC, Immunotherapy

* Correspondence: mineki@med.kawasaki-m.ac.jp
[1]Department of Immunology, Graduate School of Medicine, University of the Ryukyus, 207 Uehara, Okinawa 903-0215, Japan
[6]Present Address: Department of Microbiology, Kawasaki Medical School, 577 Matsushima, Kurashiki 701-0192, Japan
Full list of author information is available at the end of the article

Background

Human T-cell leukemia virus type 1 (HTLV-1) was the first human oncogenic retrovirus to be identified and associated with distinct human diseases such as adult T-cell leukemia (ATL) [1,2] and HTLV-1-associated myelopathy/tropical spastic paraparesis (HAM/TSP) [3,4]. HAM/TSP is a chronic progressive myelopathy characterized by spastic paraparesis, sphincter dysfunction, and mild sensory disturbance in the lower extremities [5]. In addition to neurological symptoms, some HAM/TSP patients also exhibit autoimmune-like disorders such as uveitis, arthritis, T-lymphocyte alveolitis, polymyositis, and Sjögren syndrome [6]. Major pathological features of HAM/TSP are chronic inflammation of the spinal cord, characterized by perivascular lymphocytic cuffing and parenchymal lymphocytic infiltration that includes HTLV-1-infected $CD4^+$ T cells [7]. In HAM/TSP patients, the median HTLV-1 proviral load (PVL), which reflects the *in vivo* number of HTLV-1-infected lymphocytes, is more than 10 times higher than that in asymptomatic carriers (ACs) [8]. An increase in PVL typically coincides with worsening of clinical symptoms [9]. Increased concentrations of inflammatory markers such as neopterin [10], tumor necrosis factor (TNF)-α, interleukin (IL)-6, and interferon (IFN)-γ [11], and increase in HTLV-1 antigen-specific intrathecal antibody synthesis [12] have been observed in the cerebrospinal fluid (CSF) of HAM/TSP patients. More recently, it has been reported that IFN-stimulated genes were overexpressed in circulating leukocytes and the expression correlated with the clinical severity of HAM/TSP [13]. These findings indicate that a pro-inflammatory environment, associated with increased numbers of HTLV-1-infected cells, is a characteristic immunologic profile of HAM/TSP.

OX40, also known as CD134 or TNFRSF4, is a member of the TNF co-stimulatory receptor family and is expressed on activated T cells [14]. OX40 is specifically up-regulated by the HTLV-1 viral transactivator Tax [15,16]. The ligand of OX40 (OX40L), which belongs to the TNF superfamily, was first identified as glycoprotein 34 (gp34) on HTLV-1-transformed cells [17], and it was later found to bind OX40 [18]. OX40-OX40L interactions alter the activity and differentiation of many kinds of immune cells, including regulatory T cells (Tregs), T cells, antigen-presenting cells (APCs), natural killer (NK) cells, and natural killer T (NKT) cells [14]. Previous studies have reported that OX40 is constitutively expressed in ATL cells and participate in cell adhesion [19]. Specifically, OX40 and OX40L directly mediate the adhesion of activated normal $CD4^+$ T cells, as well as HTLV-1-transformed T cells, to vascular endothelial cells [20]. Immunohistochemical staining of skin biopsy specimens from ATL patients also showed constitutive expression of OX40, suggesting its role in leukemic cell infiltration, in addition to *in vivo* cell adhesion [19].

Recent research has also shown the importance of OX40-OX40L interactions in the development of immune-mediated diseases. In particular, a strong reduction in disease severity or a complete lack of disease has been reported when OX40 or OX40L is absent or neutralized in animal models of multiple sclerosis (MS) [21], allergic asthma [22], colitis [23], diabetes [24], arthritis [25], atherosclerosis [26], graft versus host disease [27], and allograft rejection [28]. Although HTLV-1 causes an aggressive T cell malignancy (i.e., ATL) and chronic inflammatory diseases such as HAM/TSP, an association of OX40 with the inflammatory diseases observed in HTLV-1-infected individuals has not yet been established.

In this study, we investigated the expression of OX40 in HAM/TSP patients and found that the increased expression of OX40 is associated with the rapidly progressive disease. We also used an in-house monoclonal antibody (mAb) against human OX40 to test the potential of OX40 as a target molecule for immunotherapy.

Results

Tax-dependent constitutive expression of OX40 in HTLV-1-infected T cells

OX40 and OX40L have been reported to be overexpressed in HTLV-1-infected human T-cells lines [15,19,20]. These findings were obtained using northern blot or western blot analysis using whole cells; hence, our first aim was to confirm and extend these findings at the single-cell level using flow cytometry. Therefore, we used mAbs against human OX40 (clone B-7B5) and human OX40L (clone 5A8) produced in our laboratory. We analyzed six HTLV-1-infected human T-cell lines (HUT-102, MT-1, MT-2, MT-4, SLB-1, and C5/MJ). C5/MJ, SLB-1, and MT-4 cells have not been previously tested for OX40/OX40L expression. As shown in Figure 1A, expression levels were different in each cell line: OX40 was overexpressed on the surface of the Tax positive (Tax+) T-cell lines (HUT-102, MT-2, MT-4, SLB-1, and C5/MJ), but OX40 was not expressed on the surface of the Tax negative (Tax-) MT-1 cell line or the uninfected T cell line (CEM-OX40L). Consistent with previous studies, these findings suggested that OX40 expression is Tax dependent. In contrast, OX40L was not always expressed on the surface of HTLV-1-infected human T-cell lines or on the uninfected T cell line (CEM-OX40), irrespective of Tax expression (Figure 1B).

Next, we confirmed whether OX40 and OX40L protein expression on the cell surface is induced by Tax at the single-cell level by flow cytometry. We used JPX-9 cells [29], a Jurkat (HTLV-1 negative human T cell leukemia cell line) subclone generated by stable transfection of a functional Tax expression-plasmid vector, and induced Tax expression by adding $CdCl_2$ into the culture medium (final concentration: 10 μM). As shown in Figure 1C, treatment of JPX-9 cells with $CdCl_2$ induced expression of

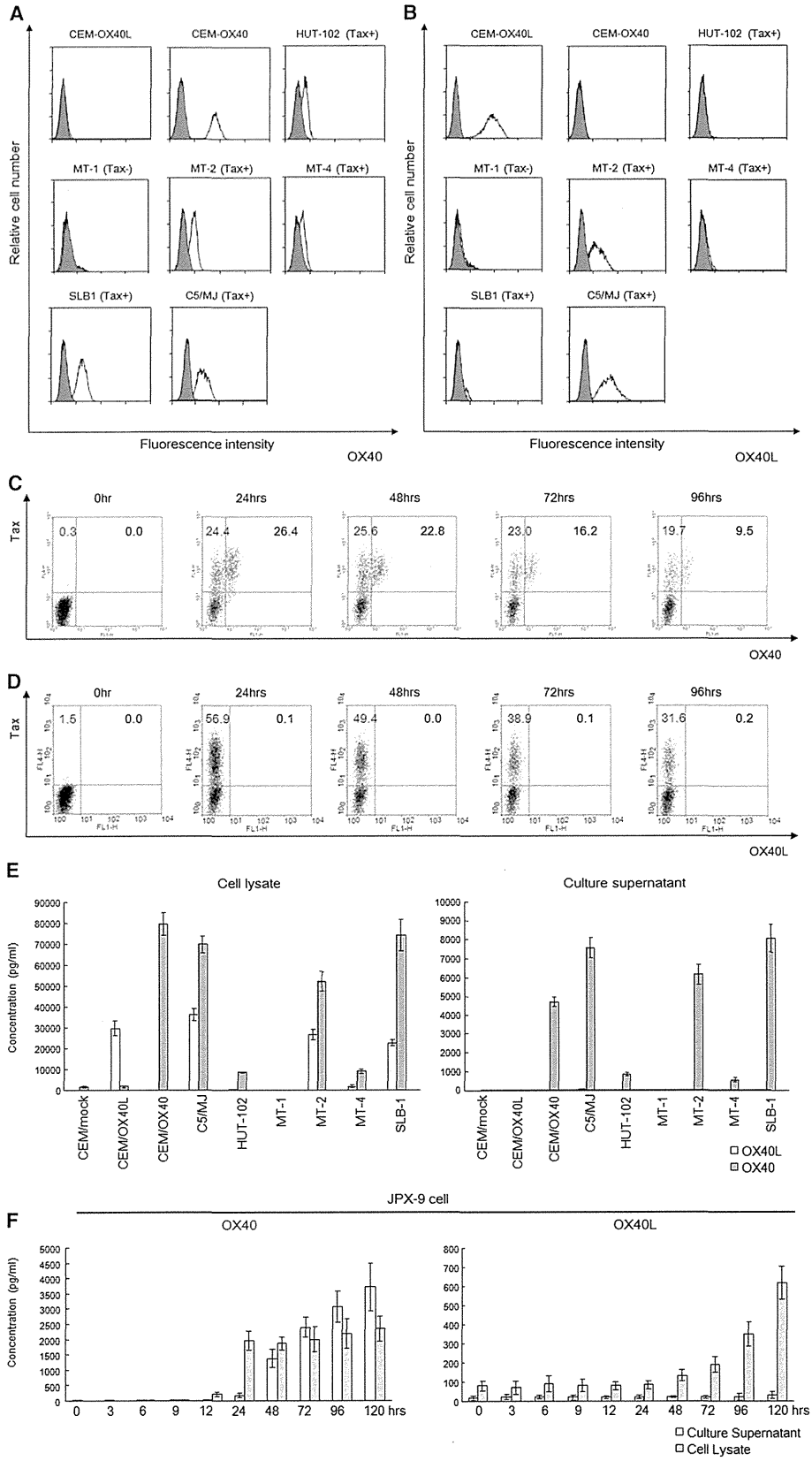

Figure 1 (See legend on next page.)

(See figure on previous page.)
Figure 1 Tax-dependent constitutive expression of OX40 in HTLV-1-infected T-cell lines and Tax-inducible JPX-9 cell line. **A.** Representative histograms of OX40 expression in 6 HTLV-1 infected T-cell lines (HUT-102, MT-1, MT-2, MT-4, C5/MJ, SLB-1) and two HTLV-1-uninfected T-cell lines (CEM-OX40L and CEM-OX40). Shaded histograms represent the isotype control. Tax+ or Tax- means whether these cells express Tax (Tax+) or not (Tax-). **B.** Representative histograms of OX40L expression in 6 HTLV-1 infected T-cell lines (HUT-102, MT-1, MT-2, MT-4, C5/MJ, SLB-1) and two HTLV-1-uninfected T-cell lines (CEM-OX40L and CEM-OX40). Shaded histograms are isotype controls. **C.** Flow cytometric analysis of expression of OX40 after induction of Tax in JPX-9 cells. **D.** Flow cytometric analysis of expression of OX40L after induction of Tax in JPX-9 cells. **E.** Soluble OX40 and OX40L levels in cell culture supernatant and cell lysate from 6 HTLV-1 infected T-cell lines (HUT-102, MT-1, MT-2, MT-4, C5/MJ, SLB-1) and three HTLV-1-uninfected T-cell lines (CEM-mock, CEM-OX40L and CEM-OX40). **F.** Soluble OX40 and OX40L levels in cell culture supernatant and cell lysate from JPX-9 cell line treated with $CdCl_2$ along with the induction of viral transactivator Tax.

Tax, and OX40 was expressed exclusively in cells that also expressed Tax. In contrast, OX40L was not expressed in JPX-9 cells even after 96 hours post Tax-induction (Figure 1D).

Previous reports indicated that the soluble forms of OX40 (sOX40) and OX40L (sOX40L) were detectable in serum of patients with autoimmune disease and cancer [30,31]. We therefore examined whether sOX40 and sOX40L levels were elevated in culture supernatants from HTLV-1 infected T-cell lines and JPX-9 cells before and after induction of Tax. In agreement with our flow cytometry data (Figure 1A), sOX40 was detected in both culture supernatants and cell lysates of Tax positive C5/MJ, HUT102, MT-2, MT-4, and SLB-1 cells (Figure 1E, gray bar). However, sOX40L was not detected in culture supernatants of any of the samples tested, but it was readily detectable in cell lysates of Tax positive C5/MJ, MT-2, MT-4 and SLB1 cells (Figure 1E, light gray bar). We next examined whether soluble OX40 and OX40L are induced by Tax in JPX-9 cells. Addition of $CdCl_2$ to the culture medium of JPX-9 cells resulted in a concomitant increase in sOX40 expression within 24 hours, indicating a strong correlation and functional link between Tax and sOX40 expression (Figure 1F, left panel). Interestingly, although OX40L was already present before induction of Tax, OX40L expression was increased after 24 hours but was never released into the culture supernatant as sOX40L within 120 hours after induction of Tax (Figure 1F, right panel).

Functional OX40 is specifically expressed on the surface of T cells naturally infected with HTLV-1 that have the potential to produce pro-inflammatory cytokines

Next, we tested whether OX40 or OX40L expression is also activated in naturally infected T cells isolated directly from HTLV-1-infected individuals. PBMCs were collected from three non-infected controls (NCs), three ACs, and four HAM/TSP patients. PBMCs were isolated from blood samples and harvested directly, or after a 16-hour in vitro cultivation in the absence of any growth factors or mitogens. After harvesting, cell samples were fixed and processed for concomitant detection of Tax, OX40, or OX40L, and CD4 expression by flow cytometry. Similar to the findings for JPX-9 cells, OX40 was detected with an anti-OX40 mAb (clones B-7B5) after 16 hours of in vitro cultivation (Figure 2A), but OX40L was not detected in cultured PBMCs from a HAM/TSP patient (HAM/TSP1) (Figure 2B). Figure 2C shows that the Tax protein was detected in $CD4^+$ T cells after cultivation. Similar to the JPX-9 cell experiments, OX40 was expressed almost exclusively in the naturally infected $CD4^+$ T cells that also expressed Tax (Figure 2D). Similar findings were observed in all samples tested, irrespective of disease status (i.e., HAM/TSP or ACs) (Additional file 1: Figure S1 and Additional file 2: Table S1). The cells from NCs did not express either OX40 or Tax in $CD4^+$ T cells, before or after cultivation (data not shown). Real time RT-PCR also showed that mRNA expression of HTLV-1 tax and OX40 in $CD4^+$ T cells was increased after cultivation, both in HAM/TSP patients and ACs (Figure 2E).

It has recently been reported [32], that the expression of another co-stimulatory member of the TNFR family, 4-1BB, is also up-regulated ex vivo in $CD4^+$ T cells from HTLV-1-infected individuals, and it was found to be correlated with Tax expression (Additional file 1: Figure S2A and B). However, the expression of OX40 is more specific for Tax^+CD4^+ cells than 4-1BB (Figure 2D and Additional file 1: Figure S2C).

Next, we sought to determine if OX40, expressed on the surface of Tax^+CD4^+ T cells from HTLV-1-infected individuals, is functional. We incubated aliquots of Fc-blocked PBMCs with biotinylated recombinant soluble OX40L at a concentration of 2.5 mg/ml for 30 min on ice. Cells were then fixed and processed for concomitant detection of Tax, CD4, and PE-streptavidin by flow cytometry. As shown in Additional file 1: Figure S3, the frequency of $CD4^+$ T cells that were positively stained with biotinylated recombinant soluble OX40L and PE-streptavidin was similar to the percentage of $CD4^+$ T cells stained by anti-OX40 mAb, indicating that these cells expressed functional OX40.

We further analyzed if $CD4^+OX40^+$ T cells in HAM/TSP patients were capable of producing the inflammatory and neurotoxic cytokines, IFN-γ and TNF-α, which, according to the bystander damage hypothesis, could cause central nervous system (CNS) inflammation and demyelination seen in HAM/TSP patients [33,34]. The frequency of pro-inflammatory cytokine positive cells within the $OX40^+CD4^+$ and Tax^+CD4^+ populations from

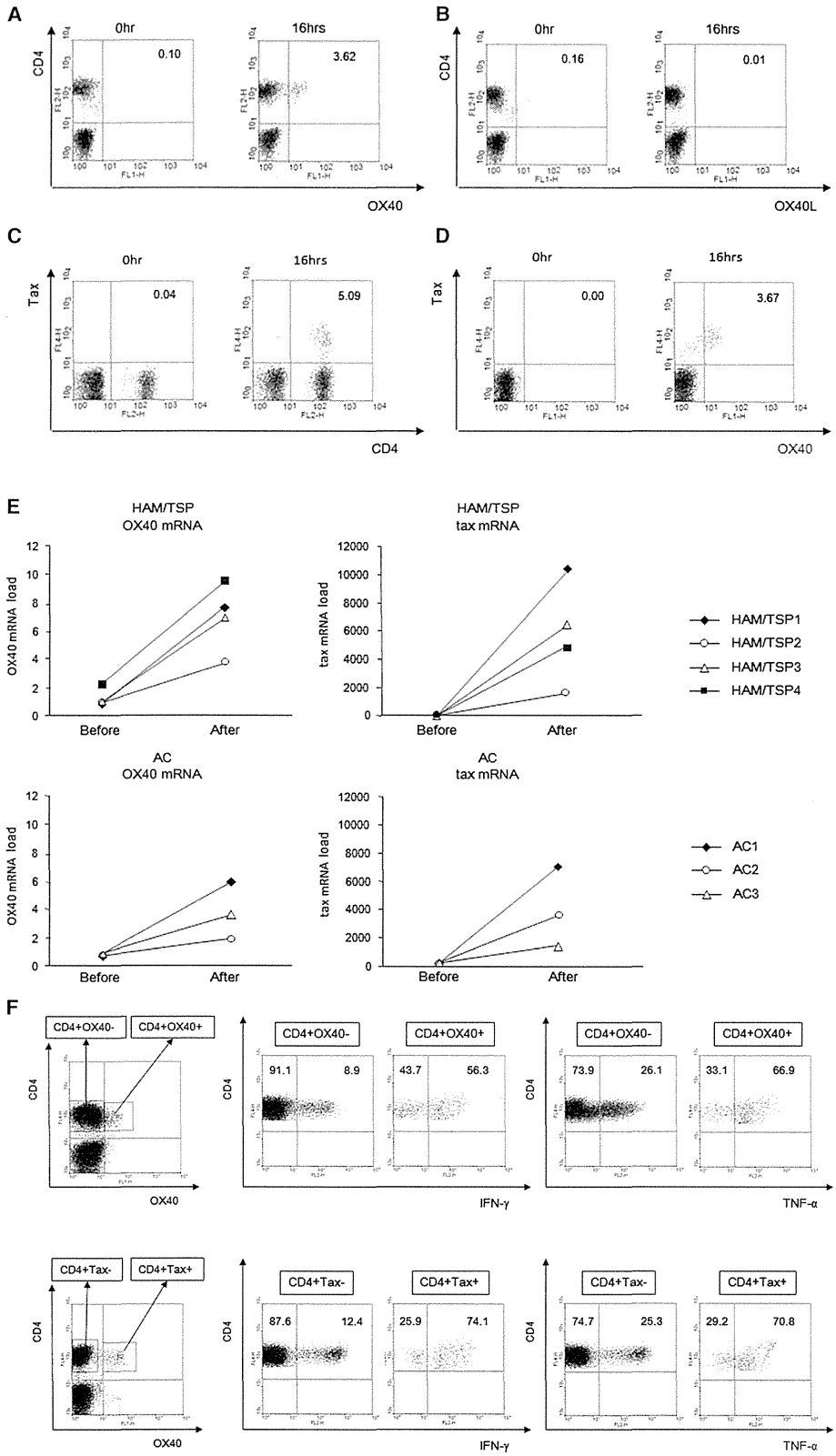

Figure 2 (See legend on next page.)

(See figure on previous page.)

Figure 2 OX40 is specifically expressed on the surface of T cells naturally infected with HTLV-1 that have the potential to produce pro-inflammatory cytokines. A. OX40 was detected on $CD4^+$ T cells of HAM/TSP patient with anti-OX40 mAb (clones B-7B5) after 16 hours *in vitro* cultivation in the absence of any growth factors or mitogen. **B.** OX40L was not detected on $CD4^+$ T cells of HAM/TSP patient with anti-OX40L mAb (clones 5A8) after 16 hours *in vitro* cultivation in the absence of any growth factors or mitogen. **C.** Tax protein was detected in $CD4^+$ T cells of HAM/TSP patient after 16 hours *in vitro* cultivation. **D.** OX40 was expressed almost exclusively in naturally infected $CD4^+$ T cells that also expressed Tax in HAM/TSP patient. **E.** Both HTLV-1 tax and OX40 mRNA expression in $CD4^+$ T cells was increased after 16 hours *in vitro* cultivation. **F.** The frequency of pro-inflammatory cytokine positive cells within the $OX40^+CD4^+$ and Tax^+CD4^+ populations from HTLV-1 infected individuals are significantly higher than $OX40^-CD4^+$ and Tax^-CD4^+ T cells, respectively ($p<0.001$, Student's t- test). One representative experiment of HAM/TSP patient (HAM/TSP1) is shown.

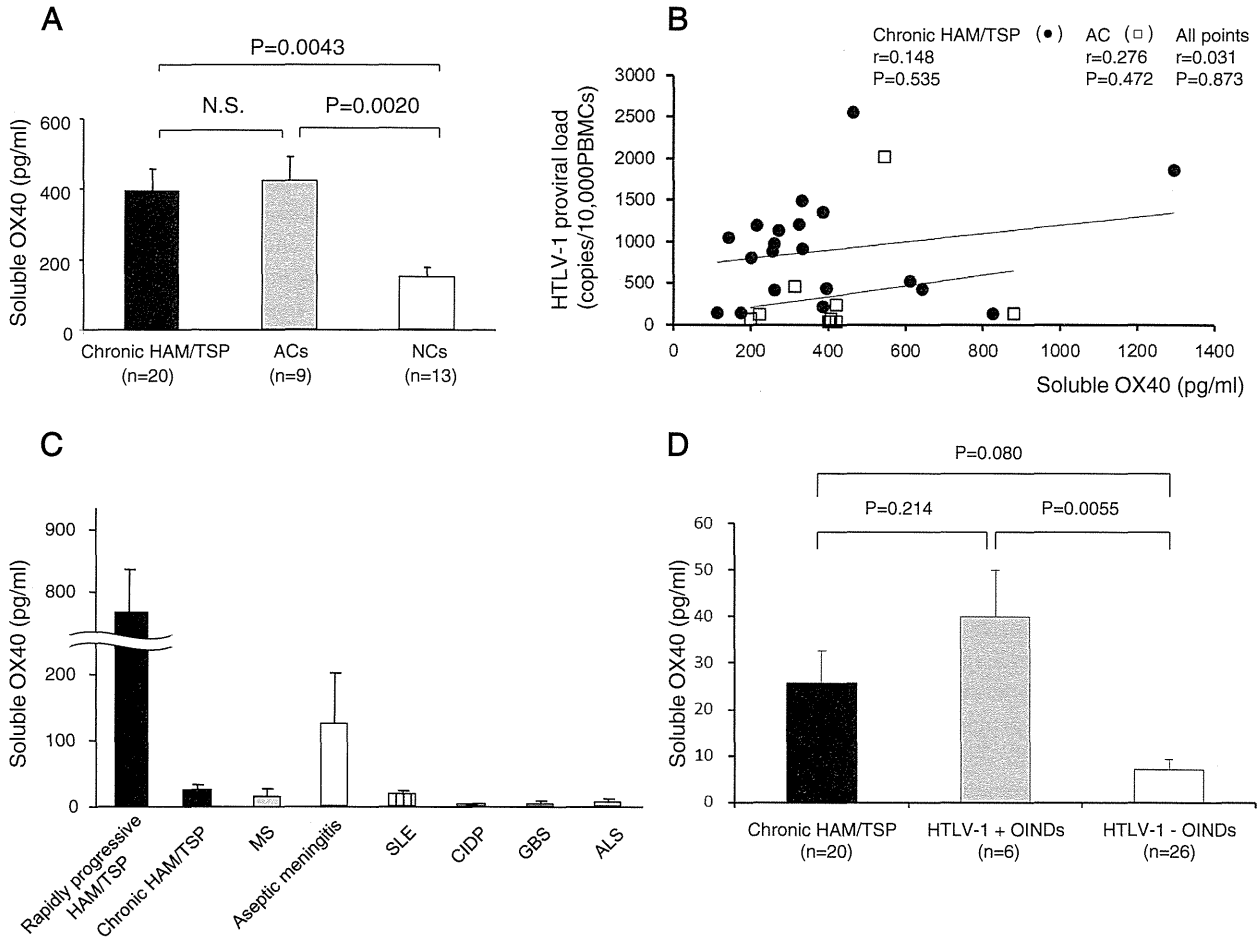

Figure 3 Increased expression of OX40 in vivo in rapidly progressive HAM/TSP patients. A. The plasma levels of soluble OX40 (sOX40) measured by ELISA. The plasma levels of sOX40 in typical HAM/TSP patients (chronic HAM: n=20), asymptomatic carriers (ACs: n=9) and normal uninfected healthy controls (NCs: n=13). **B.** No correlation between the plasma levels of sOX40 and HTLV-1 proviral load (tax copies/10,000PBMCs) from 29 HTLV-1 infected individuals (20 chronic HAM/TSP patients and 9 ACs). Data were analyzed by Spearman rank correlation. **C.** The cerebrospinal fluid (CSF) levels of sOX40 in rapidly progressive HAM/TSP patients (n=3), chronic HAM/TSP patients (n=22) and other neurological diseases including multiple sclerosis (MS) (n=12), aseptic meningitis (n=8), systemic lupus erythematosus (SLE) with neurological manifestations (n=5), chronic inflammatory demyelinating polyneuropathy (CIDP) (n=9), Guillain-Barré syndrome (GBS) (n=6), and amyotrophic lateral sclerosis (ALS) (n=9). Chronic HAM/TSP means typical cases fulfilling diagnostic criteria and rapidly progressive HAM/TSP is defined by patients' incapacity to walk unaided within three months after symptoms' onset. **D.** The levels of sOX40 in the CSF from HTLV-1 infected other inflammatory neurological diseases (HTLV-1+ OINDs), i.e. any inflammatory neurological disorders except for HAM/TSP which occurred in HTLV-1 infected individuals, was not significantly different from that of chronic HAM/TSP, whereas the levels of sOX40 from HTLV-1+ OINDs was significantly increased than that of non-infected OINDs (HTLV-1- OINDs). HTLV-1+ OINDs: 1 multiple sclerosis (MS), 1 SLE with neurological manifestations, 4 aseptic meningitis. HTLV-1- OINDs: 9 MS, 5 SLE with neurological manifestations, 7 CIDP, 5 GBS.

HAM/TSP patients are significantly higher than $OX40^-$ $CD4^+$ and Tax^-CD4^+ T cells, respectively ($p < 0.001$, Student's *t*- test) (Figure 2F and Table 1).

Increased expression of OX40 in vivo in rapidly progressive HAM/TSP patients

To investigate if OX40 expression is associated with in vivo pathogenesis of HAM/TSP, we first measured the plasma concentration of sOX40 and sOX40L in 20 chronic HAM/TSP patients, 9 ACs, and 13 NCs by ELISA by using monoclonal antibodies generated in our laboratory (Figure 3A). None of the samples had detectable levels of sOX40L (data not shown), but we could readily detect sOX40. The median level of sOX40 in NCs was 149.5 pg/ml (range 13–328 pg/ml). Significantly higher sOX40 levels were found in chronic HAM/TSP patients (median 395.2 pg/ml, range 113–1295 pg/ml) and ACs (median 423.8 pg/ml, range 201–881 pg/ml) than in NCs (p=0.0043 for differences between HAM/TSP and NCs, p=0.0020 for differences between ACs and NCs). The difference between chronic HAM/TSP patients and ACs was not statistically significant. No positive correlation was found between sOX40 in the plasma and HTLV-1 PVL in infected individuals (i.e., chronic HAM/TSP patients and ACs) (Spearman's rank correlation coefficient n=29, r=0.031, P=0.873; Figure 3B). We then tested disease specificity by measuring the levels of sOX40 in the CSF from both rapidly progressive and chronic HAM/TSP patients, and in patients with other neurological disorders, with and without inflammation (e.g., 12 MS, 8 aseptic meningitis, 5 systemic lupus erythematosus with neurological manifestations, 9 chronic inflammatory demyelinating polyneuropathy, 6 Guillain-Barré syndrome, and 9 amyotrophic lateral sclerosis patients). As shown in Figure 3C, CSF sOX40 levels were markedly increased in patients with rapidly progressive HAM/TSP (n=3) and aseptic meningitis (n=8). The CSF sOX40 levels in other HTLV-1-infected inflammatory neurological diseases, i.e. any inflammatory neurological disorders except for HAM/TSP that occurred in HTLV-1 infected individuals, (HTLV-1+ OINDs, n=6) was not significantly different from chronic HAM/TSP (n=20), whereas the sOX40 level of HTLV-1+ OINDs was significantly increased compared to non-infected OINDs (HTLV-1- OINDs, n=26; Figure 3D).

Of the HAM/TSP patients studied, paired CSF and plasma samples, i.e., blood and CSF were collected on the same day, were available for six patients. HAM/TSP patients No.10-12 had a lower concentration of sOX40 in the CSF than in the plasma (Table 2), and the patients showed a typical clinical course of HAM/TSP (i.e. slowly progressive symmetrical myelopathy) and had no history of rapid exacerbation. In contrast, HAM/TSP patients No.13-15, who had higher concentrations of sOX40 in the CSF than in the plasma, showed a rapidly progressive clinical course (i.e. patients became unable to walk within three months after onset of initial symptoms).

Expression of OX40 in inflammatory mononuclear cells in spinal cord lesions of HAM/TSP patient with short disease duration and progressive symptoms

We also examined autopsy specimens from HAM/TSP patients by immunohistochemical staining. Although there was reduced or no OX40 protein expression in HAM/TSP patients who had a long duration of illness and who no longer had active inflammation (a representative example is shown in Figure 4A), we observed marked OX40 expression in inflammatory round-shaped mononuclear cells around the blood vessels in spinal cord lesions from one HAM/TSP patient (Figure 4B). This patient (patient 1 in refs [35-38], who had a shorter disease duration of up to 2.5 years after the onset of neurological symptoms) showed predominant infiltration of $CD4^+$ T cells [36] that also expressed tax mRNA [38], pro-inflammatory cytokines [37], and matrix metalloproteinases [39]. In contrast, we observed only low background staining for OX40L in spinal cord tissues of all the HAM/TSP patients examined (a representative example is shown in Figure 4C) compared to positive control (Figure 4D).

Anti-OX40 monoclonal antibody specifically eliminated naturally infected $CD4^+$ T cells via antibody-dependent cell-mediated cytotoxicity (ADCC) in cultured PBMCs

We investigated the role of OX40 in HTLV-1 naturally infected $CD4^+$ T cells, by testing the effects of an anti-human OX40 mAb on Tax expression. As shown in Figure 5, anti-OX40 mAb (clone B-7B5) reduced the percentage of Tax-positive cells, whereas the isotype control mAb (clone 2C2: anti-HIV-1 gp21, mouse IgG1) had no effect on Tax expression (Figure 5, 1st, 2nd, and 3rd panels from left). Culture of PBMCs with anti-CD16/CD32 (Fc receptor) antibody to block Fc receptors abolished Tax suppression by anti-OX40 mAb (Figure 5, 4th panels from left), suggesting that the effect of the anti-OX40 mAb (B-7B5) is mainly mediated by ADCC. We further tested the effects of the $F(ab')_2$ fragment of anti-OX40 mAb (B-7B5) and found that the $F(ab')_2$ fragment did not suppress Tax expression; this finding supports an ADCC mechanism of action of the anti-OX40 mAb (Figure 5, right panels).

Anti-OX40 monoclonal antibody specifically eliminated OX40-positive HTLV-1 infected cells in cultured PBMCs

We examined whether suppression of OX40 expression either reduced the frequency of Tax-positive cells or selectively eliminated HTLV-1-infected cells by isolating $CD4^+$ T cells from PBMCs before and after culture, extracting genomic DNA, and measuring HTLV-1 PVL. HTLV-1 PVL in $CD4^+$ T cells was significantly reduced

Table 1 The expression of pro-inflammatory cytokines in peripheral blood mononuclear cells of HTLV-1 infected individuals

Case	Age	Sex	PVL[a]	%IFN-γ$^+$ in CD4$^+$OX40$^+$[b]	%IFN-γ$^+$ in CD4$^+$OX40$^-$	%IFN-γ$^+$ in CD4$^+$Tax$^+$[c]	%IFN-γ$^+$ in CD4$^+$Tax$^-$	% TNF-α$^+$ in CD4$^+$OX40$^+$	% TNF-α$^+$ in CD4$^+$OX40$^-$	% TNF-α$^+$ in CD4$^+$Tax$^+$	% TNF-α$^+$ in CD4$^+$Tax$^-$
HAM/TSP7	68	F	1200	56.3	8.9	74.1	12.4	66.9	26.1	70.8	25.3
HAM/TSP8	68	F	1118	77.2	5.0	91.5	4.7	84.1	10.0	87.6	10.7
HAM/TSP9	71	F	1424	64.8	4.7	80.1	5.3	70.4	18.8	80.5	16.6
mean±SE	69.0±1.0		1247±65	66.1±4.3	6.2±1.0	81.9±3.6	7.5±1.7	73.8±3.7	18.3±3.3	79.6±3.4	17.5±3.0
AC4	74	F	435	61.9	13.8	61.8	13.6	30.8	11.5	25.0	11.1
AC5	76	M	139	55.3	24.9	43.0	27.8	38.3	22.1	47.9	14.3
AC6	71	F	250	47.3	15.0	62.1	34.6	15.8	10.5	34.8	21.9
mean±SE	73.7±1.5		275±61	54.8±3.0	17.9±2.5	55.6±4.5	25.3±4.4	28.3±4.7	14.7±2.6	35.9±4.7	15.8±2.3

HAM/TSP: HTLV-1 associated myelopathy/tropical spastic paraparesis. AC: asymptomatic carrier. PVL: Proviral load.
[a] PVL: HTLV-1 tax copy number per 10^4 peripheral blood mononuclear cells (PBMCs).
[b] "%IFN-γ$^+$ in CD4$^+$OX40$^+$" means the frequency of IFN-γ$^+$ cells in the CD4$^+$OX40$^+$ cell gate.
[c] "%IFN-γ$^+$ in CD4$^+$Tax$^+$" means the frequency of IFN-γ$^+$ cells in the CD4$^+$Tax$^+$ cell gate.

Table 2 Clinical and laboratory findings of HAM/TSP patients for whom paired CSF and plasma samples were tested for soluble OX40 (sOX40)

Case	Age	Sex	Disease Duration	HTLV-1 proviral load (copies/10^4PBMCs)	HTLV-1 Ab titer (PA)	OMDS*	sOX40 (Plasma)	sOX40 (CSF)
HAM/TSP10	67	F	6 years	698	×4096	7	534.9	52.1
HAM/TSP11	29	F	1 year	1138	×16384	2	394.0	54.1
HAM/TSP12	41	F	5 years	800	×16384	4	1459.0	55.6
HAM/TSP13	62	F	1 month	224	×8192	10	626.6	752.1
HAM/TSP14	75	F	3 months	437	×4096	9	337.6	897.4
HAM/TSP15	66	F	2 months	534	×4096	9	423.5	652.5

*OMDS: Osame Motor Disability Score that graded the motor dysfunction from zero (normal walking and running) to 13 (complete bedridden): 1=normal gait but runs slow; 2=abnormal gait; 3=abnormal gait and unable to run; 4=need support while using stairs; 5=need one hand support in walking; 6=need two hands support in walking; 7=need two hands support in walking but is limited to 10 m; 8=need two hands support in walking but is limited to 5 m; 9=unable to walk but able to crawl on hands and knees; 10=crawls with hands; 11=unable to crawl but can turn sideways in bed; 12=unable to turn sideways but can move the toes.

after culture, suggesting that the anti-OX40 mAb (B-7B5) did not suppress expression of Tax but specifically eliminated OX40-positive HTLV-1 infected cells (Figure 6).

Discussion

Retroviral infection is characterized by chronic immune-system activation and pro-inflammatory cytokine production [40]. HTLV-1 infection is associated with the development of several different inflammatory conditions, including chronic arthritis, pulmonary alveolitis, polymyositis, Sjögren syndrome, and uveitis [41]. The main pathological feature of HAM/TSP is chronic inflammation of the spinal cord, characterized by perivascular cuffing of mononuclear cells accompanied by parenchymal lymphocytic infiltration. Increased spontaneous peripheral blood lymphocyte proliferation with the production of TNF-α

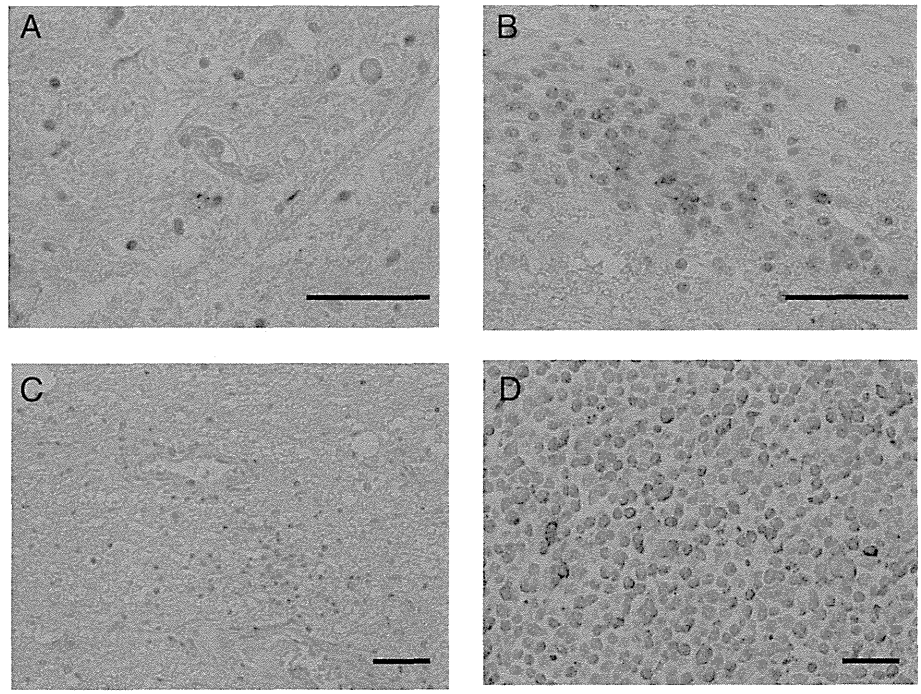

Figure 4 Expression of OX40 in inflammatory mononuclear cells in spinal cord lesions of HAM/TSP patient with short disease duration and progressive symptoms. We studied autopsy specimens from 9 HAM/TSP patients by immunohistochemical staining. **A.** No OX40 positive cells are detected in the spinal cord lesion without active inflammation of a HAM/TSP patient with a long duration of illness. Magnification: ×40. **B.** Many infiltrating mononuclear cells are positively stained by anti-OX40 mAb in the spinal cord lesion with active inflammation of HAM/TSP patient with 2.5 years of illness. Magnification: ×40. **C.** There was reduced or no OX40L protein expression in spinal cord tissues of HAM/TSP patients. OX40L showed only low background staining and there was no OX40L positive staining on inflammatory mononuclear cells in the spinal cord lesions. Magnification: ×20. **D.** Positive control staining for OX40L positive CEM-OX40L cells. Magnification: ×20. Bar: 50 μm.

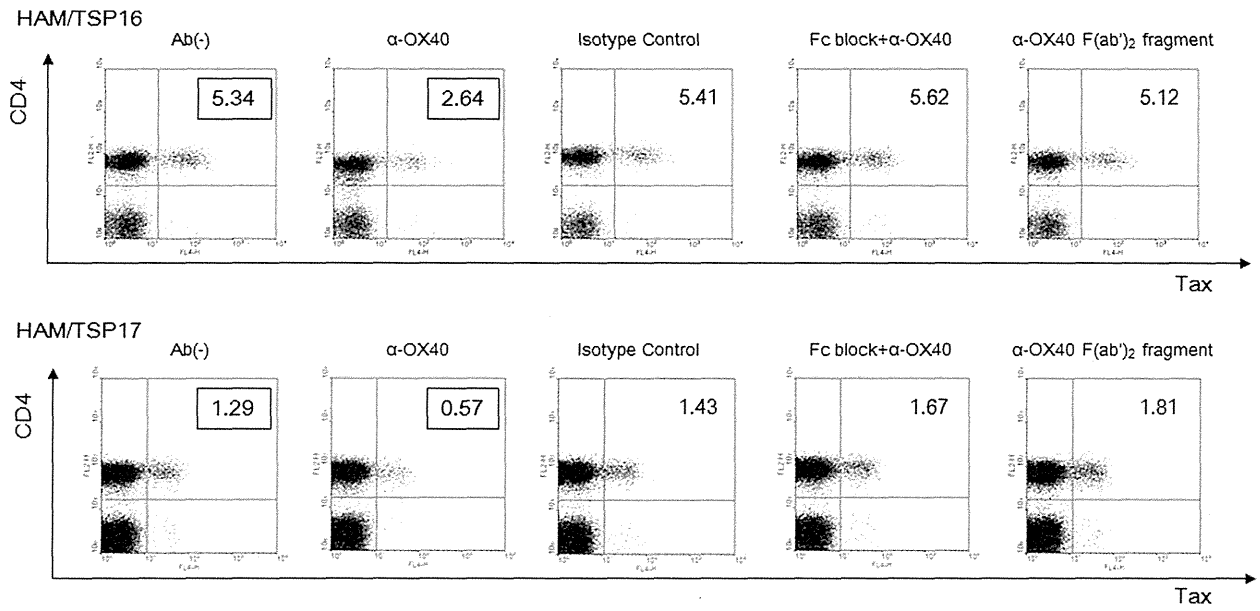

Figure 5 Anti-OX40 monoclonal antibody specifically eliminated naturally infected CD4$^+$ T cells via antibody-dependent cell-mediated cytotoxicity (ADCC) in cultured PBMCs. Anti-OX40 mAb (clone B-7B5) reduces the percentage of Tax-positive cells, whereas the isotype control mAb (clone 2C2: anti-HIV-1 gp21, mouse IgG1) has no effect on Tax expression (1st, 2nd, and 3rd panels from left). Culture of PBMCs with anti-CD16/CD32 (Fc receptor) antibody to block Fc receptors abolishes Tax suppression by anti-OX40 mAb (4th panels from left). F(ab')$_2$ fragment do not suppress Tax exppression (right panels).

and IFN-γ [42,43], high prevalence of autoantibodies, hypergammaglobulinemia, and complement fixing immune complexes have also been reported in HAM/TSP patients [6]. Recent research has shown the importance of OX40-OX40L interactions in the development of immune-mediated diseases. Specifically, a strong reduction in disease severity, or a complete lack of disease, has been reported when OX40 or OX40L is absent or neutralized in animal models. We therefore hypothesized that the OX40-positive subpopulations of chronically activated T cells exist in naturally HTLV-1-infected cells of HAM/TSP patients. These cells may function to accelerate inflammation, and blocking OX40 may have therapeutic potential in the treatment of HAM/TSP.

Previous reports indicated that OX40 is strongly stimulated by the HTLV-1 viral transactivator Tax [15,19,20]. However, these previous findings were obtained by northern blot or western blot analysis using whole cells. Thus, it was not clear if this induction occurs in naturally infected CD4$^+$ T cells of HTLV-1 infected individuals. In the present study, our flow cytometry analysis clearly showed that almost all OX40-positive cells are Tax-positive after short-term culture of naturally HTLV-1-infected cells, suggesting that OX40 is driven exclusively by Tax at the single cell level. In contrast, flow cytometry analysis of JPX-9 cells showed higher percentages of OX40$^+$Tax$^-$ cells, as well as OX40$^+$Tax$^+$ cells, after induction of Tax. Although the reasons for this discrepancy are not clear, it can be caused by differential modulation of surface and intracellular protein expression in JPX-9 cells. Our ELISA analysis indicates the existence of intracellular pools of OX40, suggesting that Tax$^+$OX40$^-$ cells also contain Tax-induced OX40 within JPX-9 cells. While the expression of another co-stimulatory member of the TNFR family, 4-1BB, has also been reported [32], our data indicate that the

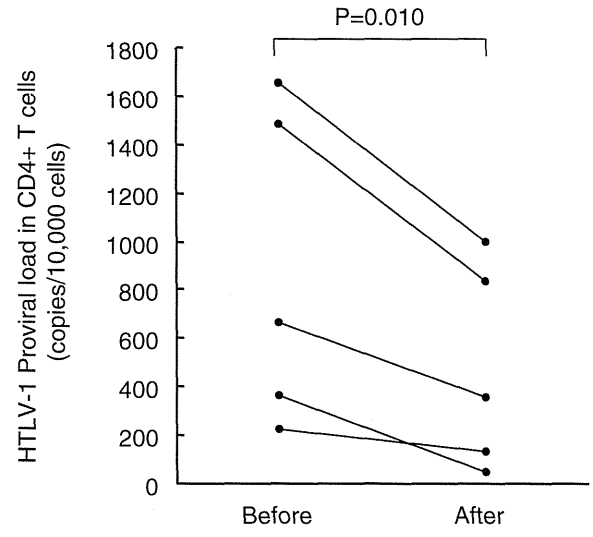

Figure 6 The HTLV-1 proviral load in CD4$^+$ T cells were significantly reduced after cultivation. CD4$^+$ T cells were isolated from PBMCs before and after cultivation, extracted genomic DNA, and measured the HTLV-1 PVL. HTLV-1 PVL in CD4+ T cells was significantly reduced after culture.

expression of OX40 was more specific than the expression of 4-1BB in Tax^+CD4^+ T cells naturally infected with HTLV-1. It has been previously reported that Tax strongly activates the 4-1BB promoter via a single NF-κB site [32] and the OX40 promoter via 2 NF-κB sites [16]; hence, sustained activation of NF-κB leads to increased expression of numerous pro-inflammatory cytokines and growth factors [44] via NF-κB signaling pathways and ultimately leads to chronic inflammation. In support of these observations, our results show that the frequencies of pro-inflammatory cytokine positive cells within the $OX40^+CD4^+$ and Tax^+CD4^+ populations from HAM/TSP patients are significantly higher than $OX40^-CD4^+$ and Tax^-CD4^+ T cells, respectively. These cells may be more likely to cross the blood brain barrier and enter the CNS, attract other cells including pro-inflammatory virus-specific $CD8^+$ cells, and result in bystander damage to the CNS tissue.

The experimental autoimmune encephalomyelitis (EAE) rat model of human MS shows a selective upregulation of the OX40 protein in encephalitogenic myelin basic protein-specific T cells in the spinal cord during onset of the disease [21]. In contrast, T cells isolated from peripheral blood and spleen of the same animal express low levels of OX40 [21]. This is similar to our present finding, where OX40 was markedly expressed in infiltrating mononuclear cells in spinal cord lesions, but not in uncultivated PBMCs from HAM/TSP patients. Because locally produced pro-inflammatory cytokines up-regulate MHC class II molecules on astrocytes and microglia, increase presentation of CNS antigens, and exert a direct cytotoxic effect on oligodendrocytes [45], the observed expression of OX40 in inflammatory mononuclear cells in spinal cord lesions suggest a role for OX40 in inflammation and neuronal damage that occurs in the CNS of HAM/TSP patients. In the rat EAE model, selective depletion of myelin-reactive T cells, by treatment with an anti-OX40 mAb-conjugated immunotoxin, effectively suppressed disease symptoms [21]. The association of clinical progression of HAM/TSP with increased HTLV-1 PVL in individual patients [9] and the strong stimulation of OX40, together with the expression of the viral transactivator Tax in $CD4^+$ T cells, indicates that targeting of OX40 positive T cells by anti-OX40 antibodies may provide a novel therapeutic strategy for the treatment of HAM/TSP.

In the present study, an anti-OX40 monoclonal antibody specifically eliminated naturally infected $CD4^+$ T cells in cultured PBMCs via ADCC. This indicates that effector cells may actively lyse HTLV-1-infected $CD4^+$ T cells that are bound by the anti-OX40 antibody. Indeed, defucosylated humanized anti-CC chemokine receptor 4 (CCR4) mAbs, which exert a strong ADCC effect, were found to be effective and well tolerated as a treatment for patients with relapsed CCR4-positive ATL or peripheral T-cell lymphoma [46]. In the present study, OX40 expression was not observed in T cells of healthy individuals, and its expression was more specific than CCR4 for HTLV-1-infected cells. This finding suggests that specific elimination of HTLV-1-infected T cells by defucosylated humanized anti-OX40 monoclonal antibodies might be a promising future approach for treatment of HAM/TSP.

We also found that plasma sOX40 levels were more elevated in HTLV-1-infected individuals (chronic HAM/TSP patients and ACs) than in NCs. Three rapidly progressive HAM/TSP patients also showed higher levels of sOX40 in the CSF than in the plasma, suggesting the possibility that sOX40 is released at high levels following strong intrathecal immune activation. In contrast, expression of OX40L was absent in HTLV-1-infected lymphocytes even after short term ex vivo cultivation, in active-chronic spinal cord lesions of HAM/TSP patient, and in plasma of HTLV-1 infected individuals. Therefore, OX40 signals might be generated by interactions with OX40L on antigen presenting cells or endothelial cells at specialized sites such as lymphoid organs. In such lesions, similar to other members of the TNF receptor superfamily like 4-1BB, sOX40 may act as an antagonist to membrane-bound receptors and induce signaling in $OX40L^+$ cells to produce cytokines, which in turn drive specific T helper (Th)-cell differentiation and suppress the generation of adaptive Tregs to participate in HAM/TSP pathogenesis.

In conclusion, we demonstrate that OX40 was specifically expressed in $CD4^+$ T cells naturally infected with HTLV-1. These cells have the potential to produce pro-inflammatory cytokines along with the expression of the viral transactivator Tax. Higher levels of sOX40 were found in the CSF than in the plasma of three rapidly progressive HAM/TSP patients, and OX40 was overexpressed in the spinal cord infiltrating mononuclear cells of HAM/TSP patient with active disease. Anti-OX40 mAb was able to specifically eliminate HTLV-1-infected $CD4^+OX40^+Tax^+$ T cells via ADCC. These findings indicate that, in addition to its established role in the regulation of T cell division and survival, OX40 may be a key molecule in the pathogenesis of HAM/TSP, as well as a potential target for immunotherapy.

Methods

Patients

Peripheral blood was studied from 23 patients with a clinical diagnosis of HAM/TSP, 9 ACs and 13 uninfected normal controls (NCs). The diagnosis of HAM/TSP was made according to the World Health Organization diagnostic criteria [47]. In this paper, chronic HAM/TSP means typical cases fulfilling diagnostic criteria and rapidly progressive HAM/TSP is defined by patients' incapacity to walk unaided within three months after

symptoms' onset. This study was approved by the Institutional Review Board of the University of the Ryukyus with license number H21-1-9. All patients provided written informed consent for the collection of samples and subsequent analysis. The CSF and plasma samples were collected before starting therapy. Control subjects of other neurological diseases were MS (n=12), aseptic meningitis (n=8), systemic lupus erythematosus (SLE) with neurological manifestations (n=5), chronic inflammatory demyelinating polyneuropathy (CIDP) (n=9), Guillain-Barré syndrome (GBS) (n=6), and amyotrophic lateral sclerosis (ALS) (n=9). The specimens were stored at −80°C until use.

Cell culture

Six HTLV-1 infected T-cell lines (HUT-102, MT-1, MT-2, MT-4, SLB-1, C5/MJ) and two HTLV-1-uninfected T-cell lines (CEM-OX40L, CEM-OX40) were used in this study. CEM-OX40 and CEM-OX40L cell lines are stable CEM-derived cell lines expressing the human OX40 or OX40L, respectively. The Tax-inducible JPX-9 cell line is a derivative of the Jurkat HTLV-1 negative human T cell leukemia cell line, which expresses biologically active Tax protein under the control of the metallothionein promoter [29]. These cells were cultured in RPMI 1640 medium supplemented with 10% heat inactivated fetal calf serum (FCS), 50 U/ml penicillin, and 50 μg/ml streptomycin (Wako) at 37°C in 5% CO_2.

Preparation of PBMC samples

Fresh peripheral blood mononuclear cells (PBMCs) were isolated on a Histopaque-1077 (Sigma) density gradient centrifugation, washed twice in RPMI 1640 with 10% heat inactivated FCS, and stored in liquid nitrogen as stocked lymphocytes until use. $CD4^+$ T cells were isolated from PBMCs by positive immunoselection with the Dynal® CD4-positive isolation kit (Invitrogen), according to the manufacturer's protocol. In brief, PBMCs were incubated with anti-CD4-coated beads for 30 min at 4°C under gentle tilt rotation. Captured $CD4^+$ cells were collected with a magnet (Dynal MPC-S) and detached from beads with DETACHaBEAD CD4/CD8® (Invitrogen). Purity was >99% $CD4^+$ T cells, as determined by flow cytometry (data not shown). To induce cytokine production by $OX40^+CD4^+$ T cells, PBMCs were cultivated for 12 hours, then 0.1 ng/ml phorbol myristate acetate (PMA) (Sigma) and 0.5 μg/ml A23187 (Sigma) and 2 mM monensin (Sigma) were added to the culture medium and further cultivated for 5 hours.

Monoclonal antibodies and reagents

We produced the following monoclonal antibodies (mAbs) in our laboratory: mouse IgG1 mAbs anti-human OX40L (clones 5A8, 8F4), anti-human OX40 (clones B-7B5 and 17D8), anti-HIV-1 p24 (clone 2C2 and NP24), and mouse IgG3 mAb anti-HTLV-1 Tax (clone Lt-4) [48] as well as rat IgG2b mAbs anti-human OX40 (clone W4-54), anti-human OX40L (clone W18) and isotype control anti-HCV (clone MO-8). Some of these mAbs were labeled using FITC, Cy5, or HRP using commercial labeling kits (Dojin or Amersham, Japan) according to the manufacturers' instructions. Biotinylated recombinant soluble human OX40L (sOX40L in a form of murine CD8-fusion protein) was purchased from Ancell (Bayport, MN) and used with PE-streptavidin (Biolegend) for staining. Recombinant human OX40 ligand/TNFSF4 and recombinant human OX40/TNFRSF4/Fc Chimera were purchased from R&D Systems (Minneapolis, MN) and used for the standard curve in sOX40L and sOX40 ELISA, respectively.

Immunohistochemistry

Immunohistochemical staining of the spinal cord specimens from HAM/TSP patients was performed on buffered formalin-fixed paraffin-embedded sections using EnVision (DAKO) method for signal detection as described previously [36]. The clinical and pathological characteristics of the patients are described elsewhere [36-39]. The monoclonal antibodies to OX40 (clone B-7B5) and OX40L (clone 8F4) were used at a final concentration of 1 μg/ml.

Flow cytometry

Cell surface staining

After thawing, cells were washed three times with phosphate-buffered saline (PBS) and fixed in PBS containing 2% paraformaldehyde (Sigma) for 20 minutes at 4°C. Fixed cells were washed with PBS containing 7% of normal goat serum (Sigma) and then incubated for 15 minutes at room temperature with various combinations of fluorescence-conjugated mAbs as follows: phycoerythrin-cyanin 5.1 (PC5)-labeled anti-CD4 (13B8.2), PC5-labeled anti-CD8 (B9.11), phycoerythrin (PE)-labeled anti-CD4 (13B8.2) (Beckman Coulter), PE-labeled anti-4-1BB (4B4) (eBioscience), fluorescein isothiocyanate (FITC)-labeled anti-OX40 (B-7B5) and OX40L (5A8). Isotype matched mouse immunoglobulins were used as a control. After the staining procedure, the cells were washed twice and analyzed by standard flow cytometry using a FACS Calibur and Cell Quest software (BD).

Concomitant detection of intracellular and cell surface molecules

For intracellular staining of Tax and/or cytokines, surface stained cells were washed and permeabilized with PBS/7% normal goat serum containing 0.2% saponin (Sigma) (PBS-SAPO) for 10 minutes at room temperature. Permeabilized cells were then washed twice and resuspended in PBS-SAPO containing FITC or cyanin 5 (Cy5)-labeled anti-Tax

mAb (Lt-4), PE-labeled anti TNF-α (BD Pharmingen) or PE-labeled IFN-γ (BD Pharmingen) mAb for 20 minutes at room temperature. Finally, the cells were washed twice and analyzed by flow cytometry.

Flow cytometry based binding assay

To determine whether cell surface OX40 is functional, aliquots of Fc-blocked cells were incubated with biotinylated recombinant soluble OX40L at a concentration of 2.5 mg/ml for 30 min on ice, followed by staining with PE-streptavidin (Biolegend) for 30 min on ice. After the staining procedure, the cells were washed twice and analyzed by flow cytometry.

ELISA

Cell lysates were prepared by lysis of 2×10^7 cells in 1ml of a lysis buffer (10 mM Tris–HCl, pH8.0, 140 mM NaCl, 3 mM MgCls, 2 mM phenylmethylsulfonyl fluoride, 0.5% Nonidet P-40) on ice for 20 min, followed by centrifugation at 13,000 × g for 10 min at 4°C. Both OX40 and OX40L levels in cell lysates, culture supernatants, plasma and CSF were assayed by in house made sandwich ELISA using monoclonal antibodies against OX40 (clone 17D8 for capture and W4-54 for detection) and OX40L (clone 8F4 for capture and W18 for detection). Briefly, 96-well Immuno Module/Strip Plates (Nunc) was coated with either anti-OX40 monoclobal antibody (clone 17D8) or anti-OX40L monoclobal antibody (clone 8F4) at 4°C overnight, then blocked with 1% casein in 0.02% thimerosal-PBS at room temperature for 30 min. After washing plates three times with wash buffer (PBS with 0.05% Tween 20, pH 7.5), 50 μl of irrelevant mouse IgG1 (anti-HIV1 p24 mAb NP24) was added into each well as a blocking antibody. OX40 or OX40L standard was diluted to 4,000 pg/ml in dilution buffer (PBS with 0.1% BSA, 0.5% Triton X100, 0.05% Tween20), and two-fold serial dilutions were performed ranged from 4,000 to 16 pg/ml. Then 50 μl of the diluted standard or samples (cell lysates, culture supernatants, plasma and CSF) were added into 96-well plates and incubated one hour at room temparature. After washing plates three times, 50 μl each of diluted (0.2 μg/μl) anti-OX40 monoclobal antibody (clone W4-54) or anti-OX40L monoclobal antibody (clone W18) conjugated to HRP was added as detection antibody and incubated for one hour at room temperature. Color reactions using alkaline-phosphatase substrate (Sigma-Aldrich) were then evaluated by Model 680 Microplate Reader (Bio-Rad) reading at 450 nm with reference at 630 nm, and the data was analyzed using the Microplate manager III software (Bio-Rad). Results are shown as mean ± SE for duplicate wells. Human interleukin-2 soluble receptor alpha (IL-2sRα) was measured by ELISA according to the manufacturer's instruction (Quantikine Human IL-2sRα Immunoassay, R&D Systems, Inc. MN).

Genomic DNA, RNA extraction and cDNA synthesis

Genomic DNA was extracted from the frozen PBMCs by QIAamp blood kit (QIAGEN, Tokyo, Japan). RNA from 1×10^5 enriched $CD4^+$ T cells was extracted using RNeasy Mini Kit with on-column DNase digestion (QIAGEN, Tokyo, Japan) according to the manufacturer's instructions. Complementary DNA (cDNA) was synthesized using PrimeScript® RT reagent Kit (Takara, Kyoto, Japan). All reaction procedures were performed as suggested by the manufacturer.

Quantification of HTLV-1 proviral load and anti-HTLV-1 antibody titers

To examine the HTLV-1 PVL, we carried out a quantitative PCR method using Thermal Cycler Dice® Real Time System (Takara, Japan) with 100 ng of genomic DNA (roughly equivalent to 10^4 cells) from PBMCs samples as reported previously [8]. Based on the standard curve created by four known concentrations of template, the concentration of unknown samples were determined. Using β-actin as an internal control, the amount of HTLV-1 proviral DNA was calculated by the following formula: copy number of HTLV-1 tax per 1×10^4PBMCs = $[(copy\ number\ of\ tax)/(copy\ number\ of\ \beta - actin/2)] \times 10^4$. All samples were performed in triplicate. Serum HTLV-1 antibody titers were determined by a particle agglutination method (Serodia-HTLV-1®, Fujirebio, Japan).

Real-Time RT-PCR analysis

We used the real-time RT-PCR method to carry out a quantitative analysis of the expression of the tax and OX40 mRNA by using Thermal Cycler Dice® Real Time System (Takara, Japan) as reported previously [49]. HTLV-1 tax or OX40 mRNA load was calculated by the following formula: HTLV - 1 tax mRNA load = value of tax/value of HPRT (Hypoxanthine Phosphorisbosytransferase). OX40 mRNA load = value of OX40/value of HPRT. We used aliquots of the same standard MT-2 cDNA preparation for all assays and the correlation values of standard curves were always more than 99%. The sequences of primers for tax mRNA detection were as follows: 5′- ATC CCG TGG AGA CTC CTC AA-3′ and 5′- ATC CCG TGG AGA CTC CTC AA-3′, and the probe that surrounded the splice junction site of tax mRNA was 5′- TCC AAC ACC ATG GCC CAC TTC CC-3′. The sequences of primers for OX40 mRNA detection were as follows: 5′-AAC CAG GCC TGC AAG CCC T-3′ and 5′-GTC CCT GTC CTC ACA GAT T-3′, and the probe that span the junction between exon 4 and 5 was 5′- ACC AAC TGC ACC TTG GCT GGG AAG CA-3′. We used the HPRT primers and probe set (Applied Biosystems) for internal calibration. All assays were performed in triplicate.